

UC Santa Barbara

UC Santa Barbara Previously Published Works

Title

s± pairing near a Lifshitz transition

Permalink

<https://escholarship.org/uc/item/0nw4p76m>

Journal

Scientific Reports, 6(1)

ISSN

2045-2322

Authors

Mishra, Vivek
Scalapino, Douglas J
Maier, Thomas A

Publication Date

2016

DOI

10.1038/srep32078

Peer reviewed

SCIENTIFIC REPORTS

OPEN

s_{\pm} pairing near a Lifshitz transition

Vivek Mishra^{1,*}, Douglas J. Scalapino^{2,*} & Thomas A. Maier^{3,*}

Observations of robust superconductivity in some of the iron based superconductors in the vicinity of a Lifshitz point where a spin density wave instability is suppressed as the hole band drops below the Fermi energy raise questions for spin-fluctuation theories. Here we discuss spin-fluctuation pairing for a bilayer Hubbard model, which goes through such a Lifshitz transition. We find s_{\pm} pairing with a transition temperature that peaks beyond the Lifshitz point and a gap function that has essentially the same magnitude but opposite sign on the incipient hole band as it does on the electron band that has a Fermi surface.

Received: 25 May 2016

Accepted: 02 August 2016

Published: 26 August 2016

The microscopic mechanism of pairing that gives rise to superconductivity in the iron based superconductors remains an unsettled issue¹. Spin-fluctuation mediated pairing^{2–4}, in which electrons form pairs by exchanging virtual $S = 1$ particle hole excitations, is a leading candidate mechanism, since superconductivity appears near the onset of a magnetic phase. However, this picture relies on the nesting properties of the electronic band structure with both hole and electron Fermi surface pockets present and the absence of hole pockets in some of the iron based superconductors^{5–11} has challenged these theories. In these systems, the hole like band drops below the Fermi energy after a Lifshitz transition^{12,13}. Nevertheless, pairing remains strong, as evidenced *e.g.* by the high T_c superconductivity reported in mono-layer FeSe films grown on SrTiO₃^{9–11,14}. Scanning tunneling microscopy experiments¹² as well as ARPES measurements^{11,13} on these FeSe mono-layers find that there are no hole pockets. Furthermore, the ARPES measurements of the variation of the gap magnitude around the electron pockets¹³ makes the possibility of *d*-wave pairing, arising from pair scattering between the electron pockets, unlikely. However, these experiments also report the existence of an incipient hole band lying 50 to 100 meV below the Fermi energy, implying that the system is just beyond a Lifshitz transition¹⁵ where the hole Fermi surface has disappeared. In addition, photoemission measurements find evidence that superconductivity occurs in the monolayer FeSe film, when SDW order is suppressed by electron doping¹¹ and density functional theory calculations¹⁶ predict that in the absence of electron doping, the ground state of the mono-layer FeSe film would have SDW order. Thus, it appears that superconductivity is induced in the FeSe mono-layer when the SDW order is suppressed by a Lifshitz transition arising from electron doping or strain¹¹. Motivated by these results, we have investigated the suppression of SDW order and the onset of superconductivity near a Lifshitz transition in a two-layer Hubbard model. This model was previously shown to have both s_{\pm} and *d*-wave pairing depending upon the strength of the interlayer hopping¹⁷. Here using this model, we show that spin-fluctuation scattering of pairs between an electron and an incipient hole band can lead to s_{\pm} pairing for a system that has undergone a Lifshitz transition.

Results

The Hamiltonian for the two layer Hubbard model that we study is

$$\begin{aligned} \mathbf{H} = & t \sum_{\langle i,j \rangle, \sigma, n} (c_{i\sigma n}^{\dagger} c_{j\sigma n} + h.c.) - t_{\perp} \sum_{i, \sigma} (c_{i\sigma 1}^{\dagger} c_{i\sigma 2} + h.c.) \\ & - \mu \sum_{i, \sigma n} c_{i\sigma n}^{\dagger} c_{i\sigma n} + U \sum_{i, n} c_{i\sigma n}^{\dagger} c_{i\sigma n} c_{i\bar{\sigma} n}^{\dagger} c_{i\bar{\sigma} n}. \end{aligned} \quad (1)$$

Here $c_{i\sigma n}^{\dagger}/c_{i\sigma n}$ creates/annihilates a fermion with spin σ on the n^{th} layer ($n = 1$ or 2). The intralayer hopping is t , the interlayer hopping is t_{\perp} and μ is the chemical potential. The band structure for this model is,

$$\xi_{\mathbf{k}} = 2t(\cos k_x + \cos k_y) - t_{\perp} \cos k_z - \mu \quad (2)$$

¹Joint Institute of Computational Sciences, University of Tennessee, Knoxville, TN-37996, USA. ²Department of Physics, University of California, Santa Barbara, CA-93106, USA. ³Computer Science and Mathematics Division & Center for Nanophase Materials Sciences, Oak Ridge National Laboratory, Oak Ridge, TN-37831, USA. *These authors contributed equally to this work. Correspondence and requests for materials should be addressed to V.M. (email: mishrav@ornl.gov)

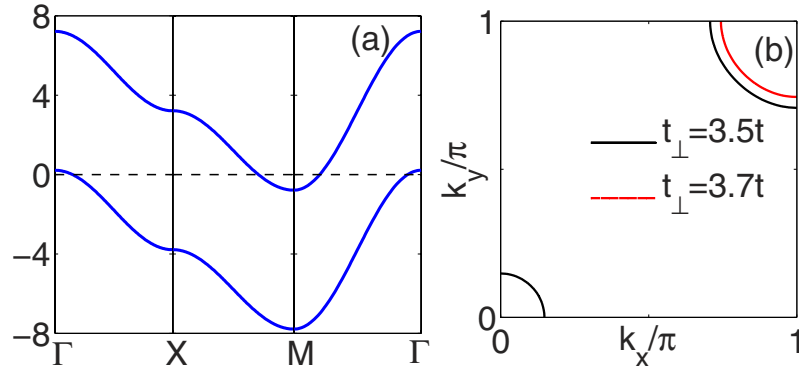


Figure 1. (a) The $k_z = 0$ and π energy bands of the two layer Hubbard model plotted along $(0, 0)$ to $(\pi, 0)$ to (π, π) to $(0, 0)$ with $t_{\perp} = 3.5t$ and the chemical potential μ adjusted for a site filling $\langle n \rangle = 1.05$. (b) The Fermi surface for $\langle n \rangle = 1.05$ with $t_{\perp} = 3.5t$ (solid black) and $t_{\perp} = 3.7t$ (red).

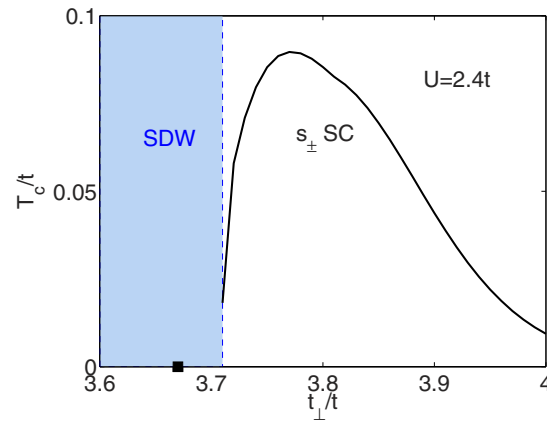


Figure 2. The s_{\pm} superconducting transition temperature T_c versus t_{\perp}/t for $\langle n \rangle = 1.05$ and $U = 2.4t$. The Lifshitz point is denoted by a filled square on the t_{\perp}/t axis and the t_{\perp}/t value where the RPA evaluated SDW instability ends by a vertical dashed line with light blue shading to the left of it.

with $t_{\perp}/t = 3.5$ and μ set so that the site filling $\langle n \rangle = 1.05$ is shown in Fig. 1(a). If the filling is kept constant as t_{\perp}/t is increased, the system has a Lifshitz transition such that for $t_{\perp} > 3.67$ the hole Fermi surface at the Γ point disappears as illustrated in Fig. 1(b). We are interested in studying the pairing for parameters such that the spin density wave (SDW) instability is suppressed by this Lifshitz transition.

In a random phase approximation (RPA) the spin susceptibility is given by

$$\chi^{RPA}(q, \Omega_m) = \frac{\chi_0(q, \Omega_m)}{1 - U\chi_0(q, \Omega_m)}, \quad (3)$$

with

$$\chi_0(q, \Omega_m) = -\frac{T}{N} \sum_{k, \omega_n} G_0(k, \omega_n) G_0(k + q, \omega_n + \Omega_m). \quad (4)$$

Here T is the temperature, $G_0(k, \omega_n) = (i\omega_n - \xi_k)^{-1}$ and $\omega_n = (2n + 1)\pi T$ and $\Omega_m = 2m\pi T$ are the usual fermionic and bosonic Matsubara frequencies. For a fixed filling, as t_{\perp}/t is increased and the Lifshitz transition is approached, χ_0 which peaks near wavevector (π, π, π) , decreases. For $\langle n \rangle = 1.05$, we take $U = 2.4t$ so that the SDW instability determined from Eq. (3) is suppressed by the Lifshitz transition as shown in Fig. 2. With this suppression of the SDW order, one can imagine that superconductivity may appear following the usual paradigm. However, the Lifshitz transition that has suppressed the SDW instability can also lead to a suppression of the s_{\pm} pairing associated with the scattering of pairs between the electron Fermi surface and the incipient hole band. For a fixed pairing strength, T_c decreases as the hole band moves below the Fermi energy¹⁸.

To explore this, we solve the Bethe-Salpeter equation

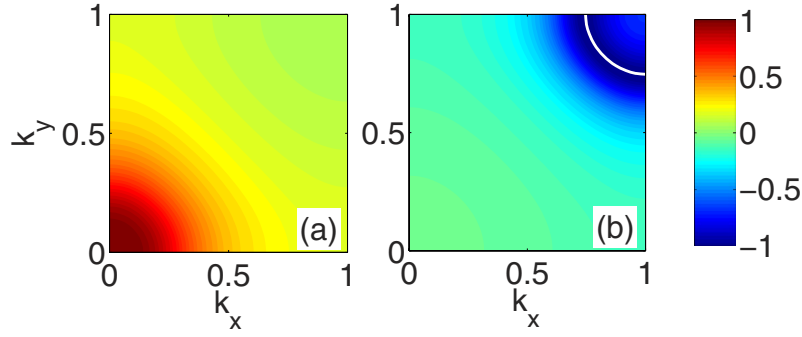


Figure 3. The momentum dependence of eigenvectors at the lowest Matsubara frequency (πT) for $\langle n \rangle = 1.05$ and $U = 2.4t$ at $t_{\perp} = 3.8t$. The eigenvector is normalized to its maximum value. The momentum dependence for the incipient hole band is shown in panel (a) and for the electron band is shown in panel (b) with the electronlike Fermi surface.

$$-\frac{T}{N} \sum_{k', \omega_{n'}} \mathbf{V}(k - k', \omega_n - \omega_{n'}) G(k', \omega_{n'}) G(-k', -\omega_{n'}) \Phi(k', \omega_{n'}) = \lambda \Phi(k, \omega_n), \quad (5)$$

and determine T_c from the temperature at which the leading eigenvalue of Eq. (5) goes to 1. Here we use a spin-fluctuation mediated interaction¹⁹,

$$\mathbf{V}(q, \Omega_m) = U + \frac{3U^2}{2} \chi^{RPA}(q, \Omega_m). \quad (6)$$

Here the first term in the effective interaction is the bare interaction U which is momentum independent. The effect of this term is small due to the sign change of the gap between the two bands. In Eq. (5) we set $G(k, \omega_n) = [i\omega_n - \xi_k - \Sigma(k, \omega_n)]^{-1}$ with

$$\Sigma(k, \omega_n) = \frac{T}{N} \sum_{k', \omega_{n'}} \mathbf{V}(k - k', \omega_n - \omega_{n'}) G_0(k', \omega_{n'}). \quad (7)$$

Note that we keep the Fermi surface unchanged in the dressed Green's function. For $\langle n \rangle = 1.05$ and $U = 2.4t$, the resulting value of T_c , interpolated from the temperature at which λ crosses 1, is plotted in Fig. 2 as a function of t_{\perp}/t . As shown in this figure, after the SDW instability is suppressed by the Lifshitz transition, a pairing transition occurs at a T_c which peaks as t_{\perp}/t increases and then falls off as the hole band is pushed further below the Fermi energy.

The momentum dependence of the superconducting gap function $\Delta(k, \omega = \pi T) \equiv \Phi(k, \pi T)/Z(k, \pi T)$ is shown in Fig. 3. This is an $A_{1g}(s_{\perp})$ state in which the sign of Δ changes between $k_z = 0$ (bonding) and $k_z = \pi$ (antibonding) bands. One can see that the magnitudes of the two gaps $\Delta(k_x, k_y, k_z = 0)$ and $\Delta(k_x, k_y, k_z = \pi)$ are comparable even though the hole band is below the Fermi energy.

In order to understand the peak in T_c that occurs as the hole band drops below the Fermi energy, it is useful to separately examine the dependence of T_c on the changes in $\chi(k - k', \omega_n - \omega_{n'})$ and $G(k', \omega_{n'}) G(-k', -\omega_{n'})$ that occur as the T_c at which the eigenvalue of Eq. (5) goes to 1 as a functional of χ and the pair propagator GG . We can calculate the variation in T_c due to the change in χ with GG unchanged when t_{\perp} increases by Δt_{\perp} ,

$$\left. \frac{\partial T_c}{\partial t_{\perp}} \right|_{GG} = \frac{T_c[\chi(t_{\perp} + \Delta t_{\perp}), G(t_{\perp})] - T_c[\chi(t_{\perp}), G(t_{\perp})]}{\Delta t_{\perp}}, \quad (8)$$

and the variation due to the change in pair propagator GG when χ is unchanged and t_{\perp} increases by Δt_{\perp} ,

$$\left. \frac{\partial T_c}{\partial t_{\perp}} \right|_{\chi} = \frac{T_c[\chi(t_{\perp}), G(t_{\perp} + \Delta t_{\perp})] - T_c[\chi(t_{\perp}), G(t_{\perp})]}{\Delta t_{\perp}}. \quad (9)$$

We set $\Delta t_{\perp} = 0.01t$. The results of the calculation are shown in Fig. 4. Here one sees that the initial increase in T_c arises from both the changes in χ and GG . The latter effect is associated with an increase in the quasi-particle spectral weight $Z^{-1}(k, \omega)$ on the electron Fermi surface that occurs as the hole band drops below the Fermi energy. This increase in the quasi-particle spectral weight initially ameliorates the decrease in T_c resulting from the submergence of the hole band. The initial positive contribution associated with the variation in χ reflects the change in the frequency structure of the spin-fluctuations. As the hole band drops below the Fermi energy, a gap opens in the low energy $q_z = \pi$ spin fluctuation spectrum and spectral weight is transferred to higher energies as shown in Fig. 5, which leads to stronger pairing²⁰. The ultimate decrease in T_c is due to the decrease of the pair

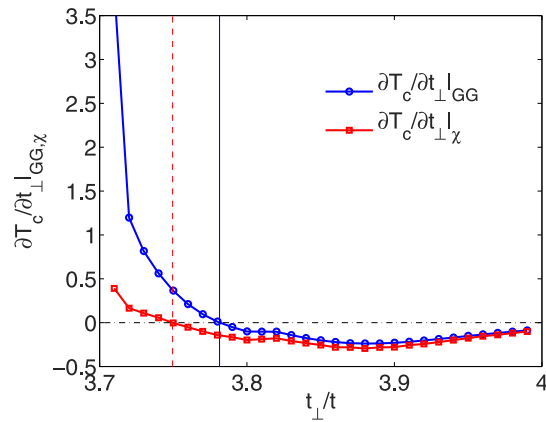


Figure 4. The variation of T_c with changes in χ (solid blue curve) and the pairfield propagators GG (dashed red curve) versus t_{\perp}/t . Here one sees that initially as t_{\perp}/t increases beyond 3.7 and the SDW order is suppressed, both the change in χ and the change in GG lead to an increase in T_c . Then, as t_{\perp}/t increases further and the hole band drops deeper below the Fermi energy, the changes in both χ and GG lead to a reduction in T_c .

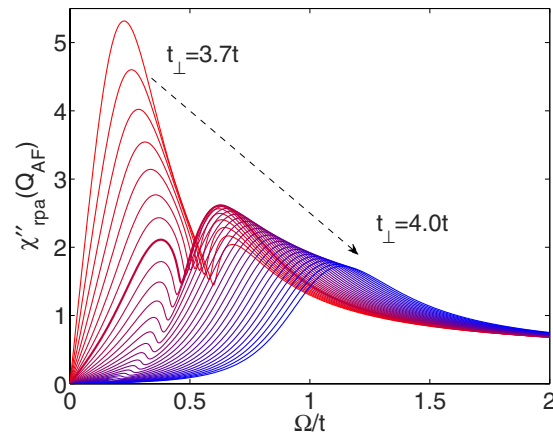


Figure 5. The imaginary part of RPA $\chi(\pi, \pi, \pi, \Omega)$ at $T = 0.1t$ versus Ω for $U = 2.4t$ for different values of t_{\perp} , which continuously increases in units of $0.01t$ from $t_{\perp} = 3.7t$ (red curve) to $t_{\perp} = 4t$ (blue curve). The thick line represents the value of $t_{\perp} = 3.77t$ corresponding to the maximum value of T_c . As t_{\perp} increases and the hole band drops below the Fermi energy, the spin fluctuation spectral weight is shifted to higher frequencies, of order 5 to $10T_c$, where it is more effective for pairing. However, as t_{\perp} increases further and the spectral weight moves to still higher frequencies, the strength of the pairing decreases and this combined with the suppression of the pair propagator GG leads to a rapid decrease of T_c .

propagator $G(k', \omega_{n'})G(-k', -\omega_{n'})$ as t_{\perp} increases and the hole band drops further below the Fermi energy, as well as the decreasing strength of the spin-fluctuations.

Discussion

To conclude, we have studied a two-layer Hubbard model with parameters chosen so that a SDW instability is suppressed by a Lifshitz transition in which the hole band at the Γ point drops below the Fermi energy. Here, we have kept the site filling fixed and varied the interlayer hopping to tune the system through the Lifshitz point. For a physical system this might be obtained via strain¹¹. Following the suppression of the SDW order, we find the onset of an s_{\pm} superconducting state whose transition temperature T_c initially increases as the system is pushed beyond the Lifshitz point by further increasing t_{\perp}/t . We find that this increase in T_c is associated with both an increase in the quasi-particle spectral weight and an increase in the strength of the pairing interaction, which are related to the incipient hole band and the resulting change in the spectral distribution of the spin-fluctuations. We find that the gap function on the incipient hole band is similar in magnitude but of the opposite sign to that on the electron band which crosses the Fermi surface.

References

1. Norman, M. R. The Challenge of Unconventional Superconductivity. *Science* **332**, 196–200 (2011).
2. Mazin, I. I., Singh, D. J., Johannes, M. D. & Du, M. H. Unconventional Superconductivity with a Sign Reversal in the Order Parameter of $\text{LaFeAsO}_{1-x}\text{F}_x$. *Phys. Rev. Lett.* **101**, 057003 (2008).

3. Kuroki, K. *et al.* Unconventional Pairing Originating from the Disconnected Fermi Surfaces of Superconducting LaFeAsO_{1-x}F_x. *Phys. Rev. Lett.* **101**, 087004 (2008).
4. Hirschfeld, P. J., Korshunov, M. M. & Mazin, I. I. Gap symmetry and structure of Fe-based superconductors. *Rep. Prog. Phys.* **74**, 124508 (2011).
5. Guo, J. G. *et al.* Superconductivity in the iron selenide K_xFe₂Se₂ (0 ≤ x ≤ 1.0). *Phys. Rev. B* **82**, 180520 (2010).
6. Mou, D. X., Zhao, L. & Zhou, X. Structural, Magnetic and Electronic Properties of the Iron-Chalcogenide A_xFe_{2-y}Se₂ (A = K, Cs, Rb, Tl and etc.) Superconductors. *Front. Phys.* **6**, 410–428 (2011).
7. Zhang, Y. *et al.* Nodeless superconducting gap in A_xFe₂Se₂ (A = K, Cs) revealed by angle-resolved photoemission spectroscopy. *Nat. Mater.* **10**, 273–277 (2011).
8. Liu, X. *et al.* Electronic structure and superconductivity of FeSe-related superconductors. *Journal of Physics: Condensed Matter* **27**, 183201 (2015).
9. Wang, Q.-Y. Interface-Induced High-Temperature Superconductivity in Single Unit-Cell FeSe Films on SrTiO₃. *Chin. Phys. Lett.* **29**, 037402 (2012).
10. He, S. Phase diagram and electronic indication of high-temperature superconductivity at 65 K in single-layer FeSe films. *Nat. Mater.* **12**, 605–610 (2013).
11. Tan, S. Interface-induced superconductivity and strain-dependent spin density waves in FeSe/SrTiO₃ thin films. *Nat. Mater.* **12**, 634–640 (2013).
12. Huang, D. Bounds on nanoscale nematicity in single-layer FeSe/SrTiO₃. *Phys. Rev. B* **93**, 125129 (2016).
13. Zhang, Y. Superconducting gap anisotropy in monolayer FeSe thin film. arxiv:1512.06322.
14. Ge, J.-F. Superconductivity above 100 K in single-layer FeSe films on doped SrTiO₃. *Nat. Mater.* **14**, 285 (2015).
15. Lifshitz, I. M. Anomalies of Electron Characteristics of a Metal in the High Pressure Region. *Zh. Eksp. Teor. Fiz.* **38**, 1569 (1960) [*Sov. Phys. JETP* **11**, 1130–1135 (1960)].
16. Liu, K., Gao, M., Lu, Z.-Y. & Xiang, T. First-principles study of FeSe epitaxial films on SrTiO₃. *Chin. Phys. B* **24**, 117402 (2015).
17. Bulut, N., Scalapino, D. J. & Scalettar, R. T. Nodeless d-wave pairing in a two-layer Hubbard model. *Phys. Rev. B* **45**, 5577 (1992).
18. Chen, X., Maiti, S., Linscheid, A. & Hirschfeld, P. J. Electron pairing in the presence of incipient bands in iron-based superconductors. *Phys. Rev. B* **92**, 224514 (2015).
19. Maier, T. A. & Scalapino, D. J. Pair structure and the pairing interaction in a bilayer Hubbard model for unconventional superconductivity. *Phys. Rev. B* **84**, 180513(R) (2011).
20. Monthoux, P. & Scalapino, D. J. Variations of T_c for changes in the spin-fluctuation spectral weight. *Phys. Rev. B* **50**, 10339 (1994).

Acknowledgements

Research sponsored by the Laboratory Directed Research and Development Program of Oak Ridge National Laboratory, managed by UT-Battelle, LLC, for the U. S. Department of Energy. DJS and TAM acknowledge the support of the Center for Nanophase Materials Sciences, a US DOE Office of Science User Facility. We acknowledge the Valinor cluster for computational resources. We thank A. Linscheid, S. Maiti, P. Hirschfeld for useful discussion.

Author Contributions

V.M., D.J.S. and T.A.M. contributed equally.

Additional Information

Competing financial interests: The authors declare no competing financial interests.

How to cite this article: Mishra, V. *et al.* s_± pairing near a Lifshitz transition. *Sci. Rep.* **6**, 32078; doi: 10.1038/srep32078 (2016).



This work is licensed under a Creative Commons Attribution 4.0 International License. The images or other third party material in this article are included in the article's Creative Commons license, unless indicated otherwise in the credit line; if the material is not included under the Creative Commons license, users will need to obtain permission from the license holder to reproduce the material. To view a copy of this license, visit <http://creativecommons.org/licenses/by/4.0/>

© The Author(s) 2016